A99-33662

AIAA 99-3639
Liquid Atomization in Multiphase Flows: A Review

G.M. Faeth
The University of Michigan
Ann Arbor, MI 48109-2140

30th AIAA Fluid Dynamics Conference
28 June - 1 July, 1999 / Norfolk, VA

Liquid Atomization in Multiphase Flows: A Review

G.M. Faeth*
The University of Michigan, Ann Arbor, Michigan 48109-2140

Abstract. Three aspects of liquid atomization (breakup) in multiphase flows are briefly reviewed: secondary breakup, turbulent primary breakup and nonturbulent primary breakup. Studies of secondary breakup have resolved aspects of breakup regimes and outcomes for shock-wave (step) disturbances when gas/liquid density ratios and effects of liquid viscosity are small but more information is needed about general drop disturbances and conditions relevant to high-pressure spray combustion where gas/liquid density ratios and effects of liquid viscosity are large. Turbulent primary breakup is caused by liquid-phase disturbances (turbulence) for practical atomization processes and for many natural phenomena; some capabilities for predicting the onset and outcomes of this breakup mechanism have been developed but important features remain to be resolved, e.g., the rate of atomization, near-surface turbulence properties, aerodynamic effects, etc. Finally, current understanding of nonturbulent primary breakup is limited due to problems of controlling liquid-phase disturbances during experiments, although recent studies show interesting relationships between turbulent liquid column breakup and secondary drop breakup; therefore, this area offers many opportunities for studies of classical primary breakup processes.

Nomenclature

C_{bs}, C_c	=	empirical coefficients
C_d	=	drag coefficient
d	=	jet exit diameter and drop diameter after breakup
d_{max}, d_{min}	=	maximum and minimum drop diameters
d_p	=	drop diameter
K'	=	empirical flow regime coefficient
L	=	injector passage length
L_c	=	liquid column breakup length
MMD	=	mass median drop diameter
Oh	=	Ohnesorge number, $\mu_f/(\rho_f d_p \sigma)^{1/2}$
q	=	momentum flux ratio, $\rho_j u_j^2/(\rho_\infty u_\infty)^2$
r	=	radial distance
Re_{ij}	=	Reynolds number based on phase i and dimension j, $u_i d_j/\nu_i$
SMD	=	Sauter mean diameter
t	=	time
t_b	=	breakup time
t_i	=	time of initiation of breakup
t_v	=	characteristic viscous time, $(\rho_f/\rho_g)\, \nu_f/u_o^2$
t^*	=	characteristic breakup time, $d_o(\rho_g/\rho_f)^{1/2} u_o$
u	=	streamwise velocity
u_p	=	drop relative streamwise velocity
v	=	cross stream velocity
v_p	=	drop relative cross stream velocity
We	=	cross flow Weber number, $\rho_\infty d_o u_\infty^2/\sigma$
We_{ij}	=	Weber number based on phase i and dimension j, $\rho_i d_j 2u_i^2/\sigma$
x	=	streamwise distance
x_e	=	streamwise location of end of surface breakup
x_i	=	streamwise location of onset of surface breakup
δ	=	liquid boundary layer thickness
λ_c	=	column wavelength

*A.B. Modine Professor, Department of Aerospace Engineering, 3000 François-Xavier Bagnoud Building, 1320 Beal Avenue, Fellow, AIAA.

λ_s	=	surface wavelength
Λ	=	radial integral length scale
μ	=	molecular viscosity
ν	=	kinematic viscosity
ρ	=	density
σ	=	surface tension
τ_b	=	characteristic secondary breakup time
τ_R	=	characteristic Rayleigh breakup time

Subscripts

cr	=	critical value for a flow regime transition
f, L	=	liquid property
g, G	=	gas property
j	=	liquid jet property
o	=	initial condition
∞	=	far from source, air jet property

Superscripts

$\bar{()}$	=	time-averaged mean property
$\bar{()}'$	=	time-averaged rms fluctuating property
$\tilde{()}$	=	mass averaged mean property

Introduction

Liquid atomization is an important classical multiphase flow problem that has received significant attention due to numerous practical applications, e.g., power and propulsion systems, among others. Liquid atomization generally is divided into primary and secondary breakup processes. Primary breakup involves the initial formation of drops and other liquid fragments at the surface of a liquid. Primary breakup is important because it controls the initial dispersion of the liquid into the gas phase and most directly connects injector design properties (hardware) and spray properties. Secondary breakup involves any subsequent breakup of drops or liquid fragments present as dispersed liquids. Secondary breakup is important because drops after primary breakup are intrinsically unstable to secondary breakup, which affects spray mixing rates due to the strong affect of drop sizes on interphase transport rates. In addition, effects of liquid heating or acceleration in the gas phase can lead to conditions where drops undergo secondary breakup. Thus, the objective of the present article is to briefly review new understanding of primary and secondary breakup based on recent studies, and to highlight aspects of these processes that merit more attention in the future. The following discussion is brief, Refs. 1-11, and references cited therein, should be consulted for additional details.

Some aspects of secondary breakup affect primary breakup; in particular, conditions can be encountered where processes of primary and secondary breakup overlap or merge. Thus, secondary breakup is considered before primary breakup in the following. In addition, due to wide variability of injector designs, exhaustive treatment of primary breakup is not feasible within the space limitations of this article. Thus, consideration of primary breakup will be limited to the classical configuration of a single round or plane liquid jet, treating primary breakup of turbulent liquid jets in still gases and nonturbulent round jets in gaseous cross flows, in turn. Griffin and Muraszew[1], Hinze,[2] Harrje and Reardon,[3] Clift et al.,[4] Lefebvre,[6] and references cited therein should be consulted for discussions of primary breakup processes of the numerous other injector configurations that are found in practice.

Secondary Breakup

Introduction

Secondary breakup is an aspect of all liquid atomization processes; therefore, it has received significant attention in the past. Early work in the field is reviewed by Giffin and Muraszew,[1] Hinze[2], Harrje and Reardon,[3] Clift et al.,[4] and Wierzba and Takayama;[5] the following discussion is limited to the recent studies of Faeth and coworkers,[12-17] as well as original sources related to these studies, e.g., Refs. 18-32. Past work generally has considered two well-defined disturbances that cause deformation and breakup of drops: shock-wave disturbances that provide step changes in the drop environment typical of drop behavior at the end of primary breakup, and steady disturbances typical of freely-falling drops. Effects of shock-wave disturbances have received the most attention due to their relevance to propulsion applications; therefore, these disturbances will be emphasized. Deformation and breakup regimes,

breakup outcomes and breakup dynamics will be considered, in turn.

Deformation and Breakup Regimes

Definitions and photographs of deformation and breakup regimes, for shock-wave disturbances, are widely available in the literature, see Refs. 2,5,19,20 and 21. When effects of liquid viscosity are small, the bag breakup regime is observed at the onset of breakup; this regime involves deformation of the drop into a disk normal to the flow, followed by deformation of the center of the disk into a thin balloon-like structure with a thicker ring at the base, both of which finally divide into drops. The shear breakup regime is observed at large relative velocities; this regime involves deflection of the periphery of the disk in the downstream direction and subsequent stripping of drops from the disk to finally leave a relatively large stable parent drop. The transition between the bag and shear breakup regime is a complex mixture of the two bounding regimes which will be called the multimode breakup regime in the following. Other regimes are known at vary large relative velocities but these regimes are not normally encountered in conventional sprays and will not be considered here.

Existing observations of secondary breakup regimes are for $\rho_f/\rho_g > 500$ and $Re > 100$, where Hinze[2] shows that breakup regimes are functions of the Weber and Ohnesorge number, We and Oh, which are proportional to the ratios of drag to surface tension and liquid viscous flows, respectively. The resulting deformation and breakup regime map is illustrated in Fig. 1. The transitions are independent of liquid viscous forces for $Oh < 0.01$ where onset of deformation (5% maximum deformation) is at $We = 0.5$, onset of bag breakup is at $We = 13$, onset of multimode breakup is at $We = 35$ and onset of shear breakup is at $We = 80$. Hinze,[2] Krzeczkowski[20] and Hsiang and Faeth,[12,13] generally agree on these transitions. Taken together, these findings plausibly suggest that deformation and breakup occur when drag forces are comparable to the stabilizing forces of surface tension if effects of liquid viscosity are small.

High pressure spray combustion involves approach toward the thermodynamic critical point where viscous forces remain finite while surface tension forces become small: this implies large Oh conditions. Rather surprisingly, the results of Fig. 1 show that drop resistance to breakup actually increases when the surface tension becomes small. Hsiang and Faeth,[14] explain this behavior by noting that the main effect of liquid viscosity is to reduce rates of drop deformation which provides more time for drop velocities to relax toward the ambient velocity at large Oh, tending to reduce the relative velocity, and thus the driving potential for drop deformation, at each stage of the deformation process. Phenomenological analysis considering this effect yielded the following relationship between We and Oh for particular deformation or breakup transitions, at large Oh:[14]

$$4We/We_{cr} = 1+4K'We_{cr}^{-1/2}(\rho_g/\rho_f)^{1/2}Oh \qquad (1)$$

where We_{cr} is the local We at the maximum deformation condition required for the transition of interest to occur and K' is an empirical factor. Values of We_{cr} and K' were fitted to Eq. (1) to yield the predicted transitions at large Oh illustrated in Fig. 1 and the resulting comparison between measurements and predictions is seen to be excellent. This behavior suggests that transition $We \sim Oh$ at large Oh, rather than the abrupt limits suggested by Hinze[2] and others, which has important implications for modeling high pressure spray combustion processes. A concern about these results, however, is that ρ_g/ρ_f for the measurements summarized in Fig. 1 are much smaller than values encountered for high-pressure sprays.

Breakup Outcomes

Assuming that breakup times and distances are small compared to characteristic times and distances in a spray, secondary breakup can be treated using jump conditions, which requires information about drop size and velocity distributions after secondary breakup. Gel'fand et al.[19] report measurements along these lines for bag breakup. Later work by Hsiang and Faeth,[12-14] provide a more complete picture of secondary breakup due to shock-wave disturbances for $\rho_f/\rho_g > 500$ and $Oh < 0.1$; therefore, some of the main findings of this research will be discussed in the following.

Numerous observations have shown that drop size distributions after secondary breakup can be represented reasonably well by the universal root normal distribution function with MMD/SMD = 1.2.[12-17] This distribution function was proposed by Simmons[29] based on extensive observations using industrial atomizers. This behavior is illustrated in

Fig. 2 for bag breakup of a variety of drop liquids. The root normal distribution function only has two moments; therefore, the entire drop size distribution is fully prescribed by SMD alone, providing a substantial simplification for compactly summarizing drop size data.

Early experiments showed that drop sizes after secondary breakup depended strongly on liquid viscosity but were independent of surface tension, in contrast to the classical drop breakup theories discussed in Hinze[2] and references cited therein where surface tension effects play a dominant role. Hsiang and Faeth,[14] used phenomenological analysis to help explain this behavior for shear breakup. This approach postulates that drops form by stripping of liquid from the parent drop. It was assumed that the relative velocity at the time of breakup can be represented by the initial relative velocity, that drop sizes after breakup are comparable to the thickness of the laminar boundary layer that forms in the liquid along the front surface of the drop due to its motion, that characteristic liquid phase velocities are on the order of $(\rho_g/\rho_f)^{1/2}u_o$, as suggested by Ranger and Nicholls,[21] and that the length of the liquid boundary layer is proportional to the initial drop diameter. Based on these ideas, the following best fit of available SMD measurements of drop sizes after secondary breakup was obtained:[14]

$$SMD/d_o = 6.2(\rho_f/\rho_g)^{1/4}(\nu_f/(d_o u_o))^{1/2} \qquad (2)$$

Available measurements of SMD after secondary breakup, along with the correlation of Eq. (2), are illustrated in Fig. 3. Remarkably, a single correlation developed for shear breakup is still effective for breakup in the bag, multimode and shear breakup regimes. The results in Fig. 3 are expressed in terms of the Weber number based on SMD after breakup. Superficially, it is evident that these Weber numbers exceed criteria for secondary breakup due to shock-wave disturbances. Additional (tertiary) breakup of these drops does not occur, however, because they have been exposed to the flow for a time and their breakup properties are represented by criteria associated with gradual disturbances, i.e., their Eötvös numbers are less than 15 which implies stable drops for gradual disturbances.[14] The correlation of Eq. (2) is seen to be reasonably effective in Fig. 3, which combined with the coefficient on the order of unity in Eq. (2) helps support the physical ideas used to develop an this expression. Finally, it is interesting that surface tension helps define conditions where secondary breakup occurs, through We, but does not affect the drop sizes that result from breakup. This behavior is similar to molecular viscosity affecting conditions where flow become turbulent through the Reynolds number but not having a significant effect on subsequent turbulent mixing rates.

Hsiang and Faeth,[13] also developed phenomenological analysis to obtain drop velocity distributions after breakup, as follows:

$$u_o/u - 1 = 2.7((\rho_g/\rho_f)^{1/2}d_o/d)^{2/3} \qquad (3)$$

Available measurements of drop velocities after bag, multimode and shear breakup are illustrated in Fig. 4 along with the correlation of Eq. (3). The measurements clearly are independent of the breakup regime and are correlated reasonably well by Eq. (3). This includes the core (parent) drops of the shear breakup regime; nevertheless, specific core drop velocity correlations are available to provide more accurate results.[14]

Breakup Dynamics

Breakup times are an important measure of the potential effectiveness of jump conditions to represent breakup processes in typical sprays; therefore, they have been measured during many past studies, see Refs. 12,13,15-17,21,26 and 27 and references cited therein. For conditions where $\rho_f/\rho_g > 500$ and $Oh < 0.1$, Liang et al.[25] show that normalized breakup times, $t_b/t^* \approx 5$ for We extending from the onset of breakup up to 10^6 (recent detailed measurements in the multimode regime, however, indicate that $t_b/t^* \approx 7$ at a local maximum between the bag/plume and plume/shear regimes at We = 40.[17] In addition, breakup times increase more systematically as Oh increases and eventually become controlled by the characteristic viscous time, t_v, which can be much larger than t*. The onset of breakup also correlates quite simply in terms of t* when $Oh < 0.1$ as $t_i/t^* \approx 2$; unfortunately, the effect of large Oh on t_i is not known.

Drops undergo significant deformation prior to the onset of breakup. They are initially drawn into flattened (oblate spheroid) shapes before the onset of breakup. Past measurements of deformations for steady disturbances, considering both gas/liquid and immuscible liquid/liuqid systems, yields the following:[14]

$$d_{max}/d_{min} = (1 + 0.07We^{1/2})^3, \quad We < 20 \qquad (4)$$

where approximate conservation of volume, $d_{min}d_{max}^2 = d_o^3$ provides the second relationship needed to define drop geometry. The limitation of Eq. (4) follows because drops shatter at We ≈ 20 for steady disturbances. These deformations also cause drop drag coefficients to increase with measurements yielding a linear variation of drag coefficient between values for a sphere, $C_d \approx 0.4$, and values for a thin disk, $C_d \approx 1.2$, as d_{max}/d_o varies in the range 1-2.[12] The combined effect of increasing cross stream dimensions and drag coefficients causes drop drag forces to increase by factors of roughly 4 and 13 at deformation conditions typical of the onset of breakup for steady and shock-wave disturbances, which has an important impact on breakup dynamics.[14]

The relatively large values of breakup times, combined with significant increases of drag forces due to drop deformation, implies that drop breakup can require appreciable times and distances compared to the characteristic times and distances of sprays, in some instances. This behavior is quantified in Fig. 5, where the motion of the parent drop, and the motion of the smallest drop formed at the onset of breakup, are plotted as a function of time for shear breakup (results for bag breakup are similar).[14,15] When normalized in the manner of Fig. 5, the density ratio, ρ_f/ρ_g is the only parameter of the problem. Thus, results are illustrated for ρ_f/ρ_g = 500 and 1000, which bound the test conditions of Refs. 14 and 15. It is evident that drops move a significant distance during breakup, up to 120 d_o, and even the parent drop moves up to 40 d_o. These distances can be a significant fraction of the spray-containing region which has motivated efforts toward treating secondary drop breakup as a rate process, rather than just by jump conditions.

In order to treat drop breakup as a rate process, the motion of the parent drop (for shear breakup) or other major liquid elements (for other breakup processes), the sizes and velocities of drops being formed, and the rate of liquid dispersion into new drops, must be known as a function of time. This is a major task and only a few studies (limited to $\rho_f/\rho_g > 500$ and Oh < 0.1) along these lines have been reported thus far, see Refs. 15-17 and references cited therein. A typical result of this work, involving the variation of the SMD of drops produced by secondary drop breakup as a function of time for shear breakup, is illustrated in Fig. 6. Measurements and predictions of phenomenological analysis of shear breakup are illustrated for the plot. These results show two types of behavior: a transient period where the boundary layer along the upstream surface of the present drop develops, yielding progressively larger drops as breakup time increases, and a quasi-steady period where the interior viscous flow of the parent drop is fully developed and the SMD becomes a fixed fraction of the parent drop diameter. Depending on conditions, given drops can spend most of their breakup time in either the transient or the quasi-steady periods. Other results show that mean drop velocities are roughly equal to parent drop velocities at each instant of time and that the rate of liquid removal from the parent drop can be correlated reasonably well in terms of an empirical clipped Gaussian function. Similar results for the bag and multimode breakup regimes (limited to $\rho_f/\rho_g > 500$ and Oh < 0.1) can be found in Refs. 16 and 17.

Conclusions

Aspects of the secondary breakup of drops have been reviewed, emphasizing breakup due to shock-wave disturbances, for various liquids at standard temperature and pressure. The main conclusions are as follows:

1. Drop deformation and breakup begin at We ~ 1 and 10, respectively, when Oh < 0.1, however, these transitions become proportional to Oh when Oh > 10. This inhibition of deformation and breakup at large Oh is important for high-pressure combustion processes where Oh becomes large when the drop surface approaches the thermodynamic critical point.

2. Drop-size distributions after secondary breakup satisfy the universal root normal distribution function with MMD/SMD = 1.2 due to Simmons,[29] similar to other observations in sprays.[29] Thus, the drop-size distribution after secondary breakup is completely defined by the SMD alone.

3. Jump conditions for drop sizes and velocities after secondary breakup can be correlated quite simply based on phenomenological theories. Remarkably, drop sizes are strongly affected by liquid viscosity but not by the surface tension, even though secondary breakup regimes are strongly affected by the surface tension but not by the liquid viscosity.

4. Secondary breakup requires significant times and distances and cannot be properly represented by jump conditions in some instances. A few studies of drop breakup properties as a function of time have been reported,[15-17] but much more work along these lines must still be done in order to treat secondary breakup when jump conditions cannot be used.

Except for the deformation and breakup regime map, existing information about secondary breakup is mainly limited to shock-wave disturbances in air at standard temperature and pressure Effects of other types of disturbances, and both ρ_f/ρ_g and Oh, must be resolved in order to better understand the secondary breakup properties of practical sprays. Finally, understanding of the temporal properties of secondary breakup is very limited and more information must be developed to treat the numerous practical applications where secondary breakup must be treated as a rate process rather than by jump conditions.

Turbulent Primary Breakup

Introduction

Primary breakup to form drops near liquid surfaces is an important spray process because it initiates atomization, provides the initial conditions for predictions of spray structure and it is the process where the designer modifies hardware to achieve specific objectives. Unfortunately, current understanding of primary breakup is limited due to problems of observing primary breakup in dense spray environments near liquid surfaces, effects of secondary breakup and interphase transport that modify drop properties prior to drops reaching conditions where their properties can be measured readily, and effects of flow development and liquid disturbances (turbulence) at the jet exit that have an unusually large impact on primary breakup properties. Advances in measurements methods, however, have contributed to progress in gaining a better understanding of primary breakup. Two simple and classical examples of this work will be discussed in this article, both involve pressure atomized primary breakup in still gases in this section and nonturbulent primary breakup in cross flowing gases in the next section. The following discussion of turbulent primary breakup in still gases will consider breakup onset and end, breakup otcomes and liquid breakup lengths, in turn.

Breakup Onset and End

Numerous studies of pressure-atomized sprays have established that primary breakup properties are strongly affected by the degree of flow development and the presence of turbulence at the jet exit. For example, De Juhasz et al.[33] and Lee and Spencer[34,35] showed that atomization quality differed for laminar and turbulent flow at the jet exit and postulated a unique turbulent primary breakup process for turbulent liquid jets in still gases. Numerous later studies supported these findings.[36-37] Such behavior is not surprising, however, in view of the widely recognized importance of jet exit conditions on the properties of single-phase jets.[58-60] In fact, past studies show that primary breakup can be suppressed entirely for injection into still air at STP by using supercavitating flows where the liquid jet separates from the passage wall near the end of the contraction section and does not reattach in order to provide uniform and nonturbulent velocity distributions at the jet exit, see Karasawa et al.[61] This behavior is also expected because similar flows are widely used to prevent liquid breakup for liquid jet cutting systems.[62] Finally, aerodynamic effects have little effect on drop properties after primary breakup of pressure atomized turbulent liquid jets in still gases at STP, aside from well-defined exceptions to be discussed later.[46,47,50-52] In particular, effects of liquid/gas-density ratio on liquid breakup, expected based on classical aerodynamic breakup theories,[63,64] were not observed for $\rho_f/\rho_g < 500$; instead, primary breakup properties were largely controlled by flow properties at the jet exit.[51-52]

Wu et al.[52] report a study of turbulent primary breakup where the degree of flow development at the jet exit was controlled so that its effect on primary breakup properties could be examined. These experiments involved pressure-atomized jets provided by a converging passage having a large contraction ratio and shaped to yield a nonturbulent uniform flow at its exit. The degree of flow development at the jet exit was then controlled by removing the boundary layer formed along the walls of the converging passage and providing constant-diameter passages of various lengths after boundary layer removal. Some typical pulsed shadowgraphs of the flow near the jet exit are illustrated in Fig. 7 for water injected into still air at STP with Re_{fd} = 260,000. Two conditions are shown: a nearly nonturbulent jet exit condition with a

very short constant-area passage (L/d = 0.5) and a nearly fully developed turbulent exit condition with a long constant area passage (L/d = 10.0). The vortical flow for the turbulent jet exit condition produces ligaments at the liquid surface which break up into drops close to the jet exit; in contrast, the nonturbulent jet exit condition results in suppression of ligament formation and primary breakup, yielding a smooth-surfaced liquid stream similar to liquid cutting jets.[62] These experiments indicated the appearance of turbulent primary breakup for L/d > 4-6 and Re_{fd} > 10,000-40,000 for nonturbulent conditions at the contraction exit with the results of Grant and Middleman[37] indicating the presence of turbulent primary breakup for Re_{fd} > 3000 in the presence of strong inlet disturbances. More study of effects of jet exit properties on primary breakup is needed but these results strongly suggest that measurements of the atomization properties of short L/d pressure-atomized injectors in still gases at STP are dominated by effects of inlet and contraction disturbances as well as turbulence generated near the reattachment point of separated flows.

Given that jet exit conditions are turbulent, the next issue is to determine the position of the liquid surface where turbulent primary breakup occurs. For example, the flash photograph of turbulent jet exit conditions in Fig. 7 shows that drops do not begin to form until some distance from the jet exit, which is generally the case, whereas conditions are also observed where drop formation ends at some point along the liquid surface, see Ref. 57. Phenomenological analyses have been used to define conditions for the onset and end of turbulent primary breakup along the surface of the turbulent liquid jet.[49-52] These analyses assumed that drops are formed from turbulent eddies when the kinetic energy of the eddy is comparable to the surface energy required to form a drop of comparable size, that the spectral ranges of interest for the turbulence includes the large-eddy and inertial subranges (experiments to date have been limited to the formation of drops much larger than Kolmogorov length scales), that aerodynamic effects are small, and that growing disturbances in the liquid surface convect with the mean streamwise velocity at the jet exit for the Rayleigh breakup time required to form a drop from a ligament of given size. Correlations of the streamwise distances for the onset and end of turbulent primary breakup of round liquid jets in still gases, based on these ideas, are illustrated in Fig. 8, along with best fit of the available measurements, as follows:

$$x_i/d = 2000\, We_{fd}^{-0.67} \qquad (5)$$

$$x_e/d = 0.0000158\, We_{fd}^{1.68} \qquad (6)$$

Liquid breakup length results also shown on the plot will be discussed later. Notably, the predicted powers of We_{fd} for the onset and end of surface breakup are –0.4 and 2.0; thus, while the empirical powers of Eqs. (5) and (6) differ from these predictions, the differences are not large in view of the approximation of the theories and the uncertainties of the measurements. The magnitude of the coefficients of Eqs. (5) and (6) are also reasonable for the processes considered.[51] Thus, the results illustrated in Fig. 8 yield the following breakup regimes with increasing We_{fd}: (1) only breakup of the liquid column as a whole, (2) onset and end of turbulent primary breakup along the surface followed by breakup of the liquid column as a whole, and (3) onset of turbulent primary breakup followed by breakup of the liquid column as a whole. The first of these regimes corresponds to the classical definition of first wind-induced breakup whereas the remaining regimes correspond to the classical definitions of second wind-induced and atomization breakup (depending on the distance from the jet exit where the onset of breakup occurs).[4,7] In the present instance, however, the classical definitions are clearly misnomers because no aerodynamic effects are involved in any of the results illustrated in Fig. 8. Aerodynamic effects on the onset and end of turbulent primary breakup can occur, however, when ρ_f/ρ_g < 500, see Ref. 50 for a discussion of these results.

Breakup Outcomes

Measurements of drop size and velocity distributions after various turbulent primary breakup processes have also been reported.[49-56] Similar to findings for secondary breakup, drop sizes after turbulent primary breakup satisfy the universal root normal distribution with MMD/SMD = 1.2 and can be completely specified by the SMD alone. The variation of SMD along the liquid surface was initially studied for ρ_f/ρ_g > 500 where aerodynamic effects are small.[49] Phenomenological analysis was used to interpret these data similar to the approach used for x_i and x_e. It was assumed that the SMD was proportional to the largest drop that could be formed at a particular position, based on convection and Rayleigh breakup of

similarly sized ligaments as discussed earlier, that all smaller sized ligaments are not present because they have decayed away, and that all larger sized ligaments have not had sufficient time to form drops. Available measurements of the variation of SMD with distance along the liquid surface are plotted as suggested by this theory in Fig. 9. Measurements and theory are in good agreement, yielding the following best-fit correlation:

$$SMD/\Lambda = 0.65(x/(\Lambda We_{f\Lambda}^{1/2}))^{2/3} \qquad (7)$$

The powers of Eq. (7) follow directly from the theory, and the coefficient is of order unity as expected, which suggests that the physical principles used to derive the equation are reasonable. Unlike secondary breakup, where the SMD is strongly affected by liquid viscosity, the SMD after turbulent primary breakup is independent of liquid viscosity. Drop sizes are seen to progressively increase with increasing distance from the jet exit and approach the diameter of the liquid column itself for conditions where breakup of the entire liquid column occurs, based on the correlation of Grant and Middleman[37] illustrated in Fig. 8. This provides a plausible physical mechanism for the breakup lengths of turbulent liquid jets that will be discussed subsequently.

Similar to criteria for the onset and end of turbulent primary breakup along liquid surfaces, aerodynamic effects can influence drop sizes after turbulent primary break for $\rho_f/\rho_g < 500$. This behavior follows because the characteristic Rayleigh breakup times of ligaments, τ_R, increase more rapidly with increasing ligament size than the characteristic secondary breakup times of ligaments, τ_b. This implies a tendency for primary and secondary breakup of ligaments to merge for turbulent primary breakup as distance from the jet exit increases, causing the resulting SMD to drop below the correlation illustrated in Fig. 9. Analysis of these conditions was carried out using Eq. (7) to define initial drop sizes and then applying the secondary breakup result of Eq. (2) to obtain the final SMD after merged primary and secondary breakup. The resulting best fit correlation of merged primary and secondary breakup is as follows:[50]

$$\rho_g SMD u_o^2/\sigma = 12.9(x/\Lambda)^{1/3}$$
$$(\rho_g/\rho_f)^{3/2} W_{f\Lambda}^{5/6} Re_{f\Lambda}^{-1/2} \qquad (8)$$

where Eq. (8) should be used when $\rho_f/\rho_g < 500$ and

$$\tau_R/\tau_b = (\rho_f/\rho_g)^{1/2}(xWe_{f\Lambda}/\Lambda)^{1/3} > 4 \qquad (9)$$

Available measurements of drop sizes after merged primary and secondary breakup are illustrated in Fig. 10 along with the correlation of Eq. (8). The agreement between measurements and correlations is very good and the coefficient of Eq. (8) has a reasonable magnitude, tending to support the physical ideas used in its derivation. Corresponding ways to handle aerodynamic effects on the onset of turbulent primary breakup are discussed in Ref. 50.

Typical mass-averaged streamwise and cross stream velocities after turbulent primary breakup at the surface of round liquid jets are plotted as a function of distance from the jet exit in Fig. 11. Results at $\rho_f/\rho_g >$ 500 are shown as open symbols while those at $\rho_f/\rho_g <$ 500 are shown as filled and half-filled symbols to highlight potential aerodynamic effects. Except for a small region near the jet exit, where the effect of the passage walls retards streamwise velocities, $\tilde{u}_p/\bar{u}_o \approx 0.9$ and $\tilde{v}_p/\bar{u}_o \approx 0.06$, relatively independent of position. Noting that the maximum values of $\bar{v}_o'/\bar{u}_o \approx 0.06$ for fully-developed turbulent pipe flow, see Hinze,[59] it is concluded that mass-averaged streamwise and cross stream drop velocities after turbulent primary breakup correspond to streamwise velocities and rms cross stream velocity fluctuations in the liquid jet, respectively. Exceptions include reduced rms cross stream velocities as the tip of the liquid jet is approached due to flapping of the entire liquid column,[56] and a trend toward reduced streamwise velocities at small ρ_f/ρ_g, which suggests potential aerodynamic effects for high pressure sprays. Finally, drop size distributions of turbulent primary breakup have been found to be uniform at each point along the liquid surface.[56]

Liquid Breakup Lengths

The breakup length of turbulent liquid jets in still gases of interest for spray modeling efforts because the breakup location signals conditions where the dispersed multiphase flow regime is reached. Liquid breakup lengths also are of interest for gaining insight about the properties of turbulent primary breakup along liquid surfaces. Past studies of the length of turbulent liquid jets in still gases are mainly limited to round jets and include the experimental

studies of Chen and Davis,[36] Grant and Middleman,[37] Phinney,[38] Wu and coworkers,[49-52] Sallam et al.[56,57] and references cited therein. Using available data, Grant and Middleman,[37] developed a reasonably effective correlation of mean liquid jet breakup length, based on dimensional analysis, as follows:

$$L_c/d = 8.51We_{fd}^{0.32} \quad (10)$$

This expression has already been encountered during the discussion of Figs. 8 and 9. Subsequently, Wu and coworkers,[49-52] reported a more mechanistic approach to find L_c/d, noting that the correlation of Grant and Middleman,[37] illustrated in Fig. 9 corresponds to conditions where the diameter of drops formed by turbulent primary breakup was comparable to the diameter of the liquid jet itself when aerodynamic effects were negligible. Applying this concept in conjunction with the drop size relationship for turbulent primary breakup given by Eq. (7) then yields:[57]

$$L_c/d = C_cWe_{fd}^{1/2} \quad (11)$$

where C_c is an empirical parameter on the order of unity. Equation (11) is very similar (aside from some difference in the power of We_{fd}) to the empirical Grant and Middleman[37] correlation of Eq. (10), which is encouraging. Nevertheless, there are two major concerns about these expressions: what are the potential aerodynamic effects (analogous to the merging of primary and secondary breakup along the surface) and what are the potential effects of weakly-developed turbulence when jet exit Reynolds numbers are small?

Sallam et al.[57] have recently considered the breakup lengths of round turbulent liquid jets in still air at STP in an effort to resolve potential aerodynamic and low jet exit Reynolds number effects. Their observations showed when values of We_{fd} exceeded the upper end of the data range considered by Grant and Middleman[37] the turbulent liquid column breakup mechanism changes. Then, large-scale turbulence distorts the liquid column to a significant degree, placing much of it in cross flow, and leading to the formation of bag-like and shear-like structures analogous to structures observed during the secondary breakup of drops and the primary breakup of nonturbulent liquid jets in cross flows (denoted bag/shear breakup). This behavior implies a surprising aerodynamic effect on breakup of the liquid column as a whole for $\rho_f/\rho_g > 500$; namely, as transition to nonturbulent liquid column breakup in cross flow as opposed to an effect related to the merging of primary and secondary breakup that was discussed in connection with Fig. 10 for $\rho_f/\rho_g < 500$.

Sallam et al.[57] present a simplified phenomenological analysis of bag/shear breakup. This involves assuming that the time of breakup for a nonturbulent liquid jets in cross flow can be expressed similar to the secondary breakup times of drops, as a multiple of t* independent of the breakup regime, and that the point of breakup corresponds to the streamwise distance reached by the column while moving at the mean jet exit velocity for this breakup time. These ideas yield the following expression for the bag/shear breakup length of a turbulent liquid jet:[57]

$$L_c/d = C_{bs}(\rho_f/\rho_g)^{1/2} \quad (12)$$

Measurements from Chen and Davis,[36] Grant and Middleman[37] and Sallam et al.[57] were used to establish expressions for round liquid column breakup lengths as illustrated in Fig. 12. Several correlations of the measurements are shown on the plots, as follows: (1) the correlation of Eq. (10) due to Grant and Middleman[37] based on measurements with We_{fd} of 10^2-10^5, (2) the best-fit correlation of turbulent breakup theory based on Eq. (11),

$$L_c/d = 2.1We_{fd}^{1/2} \quad (13)$$

for measurements with We_{fd} of 700-30,000; and (3) the best-fit correlation of bag/shear breakup based on Eq. (12)

$$L_c/d = 11.0(\rho_f/\rho_g)^{1/2} \quad (14)$$

for measurements with We_{fd} greater than 100,000 (and correlations for both ethanol/air and water/air flows). The measurements are in excellent agreement when they can be compared and the Grant and Middleman[37] correlation is effective over the range of We_{fd} that they considered. Closer examination, however, shows that this performance is an artifact of transition from laminar to turbulent breakup at small We_{fd} (where Reynolds numbers vary in the range 5000-25,000) and from turbulent to bag/shear breakup at large We_{fd} (where effects of liquid/gas density ratio are small for the test conditions of Fig. 12 and all involve $\rho_f/\rho_g >$ 500).[47] The combined correlations all seem quite reasonable with C_c of Eq. (11) and C_{cs} of Eq. (12) on

the order of unity as expected. In addition, C_{cs} of Eq. (12) is also close to the values found by Hiroyasu et al.[39] and Chehroudi et al.[40] for liquid breakup lengths measured using practical pressure-atomized injectors injecting into high-pressure gases. This latter behavior may be fortuitous, however, because the jet exit turbulence states of Refs. 39 and 40 are not well defined and the shorter L_c/d observed at high pressures (where $\rho_f/\rho_g < 500$) probably involves effects of merging of primary and secondary breakup similar to the results of Fig. 10 which is very different from the bag/shear breakup mechanism of the entire liquid column characteristic of the results of Fig. 12.

Conclusions

Aspects of turbulent primary breakup have been reviewed, emphasizing the classical pressure-atomization process involving single round or plane liquid jets in still gases. The main conclusions are as follows:

1. The turbulent primary breakup process postulated by De Juhasz et al.[33] nearly 70 years ago dominates pressure atomization for $\rho_f/\rho_g > 500$, which includes most pressure atomization processes in still air at STP. At these conditions, uniform nonturbulent liquid jets in still gases behave similar to liquid cutting jets and do not break up within distances of interest for most practical atomization processes. While there is significant understanding of turbulent primary breakup for fully-developed turbulent pipe flow (large L/d) at the jet exit, there is virtually no information available concerning turbulent primary breakup for the partially turbulent and nonuniform flows (small L/d) typical of most practical injectors.

2. Drop-size distributions after turbulent primary breakup approximate the universal root normal distribution with MMD/SMD = 1.2 due to Simmons,[29] similar to other observations in sprays,[7,9] and are completely defined by the SMD alone. Drop velocity distributions after turbulent primary breakup approximate uniform distributions.

3. Drop properties and the locations of the onset and end of turbulent primary breakup along liquid surfaces can be explained by equating the surface tension energy to form drops to the kinetic energy of corresponding turbulent eddies within the large-eddy and inertial ranges of the turbulence spectrum. Similarly, drop sizes after turbulent primary breakup can be explained by associating the SMD with the largest drops that have sufficient residence time in the flow to be formed at the point in question by Rayleigh breakup of protruding ligaments. Finally, mean drop velocities after turbulent primary breakup approximate mean velocities and rms velocity fluctuations in the liquid in the streamwise and cross stream directions, respectively.

4. The presence of aerodynamic phenomena for turbulent primary breakup largely is governed by the liquid/gas density ratio. When $\rho_f/\rho_g < 500$, aerodynamic phenomena influence conditions at the onset of breakup, drop sizes after breakup and drop velocities after breakup (to a lesser extent). Phenomenological theories are available to help explain aerodynamic enhancement of breakup onset and of drop sizes after breakup, the latter involving merging effects of primary breakup and secondary breakup of ligaments.

5. Significant information about turbulent liquid breakup lengths is available for $\rho_f/\rho_g > 500$. At moderate We_{fd}, liquid jet breakup is associated with the turbulent primary breakup mechanism where liquid column breakup occurs when drop sizes due to turbulent primary breakup are comparable to the diameter of the liquid column itself. At large We_{fd}, however, liquid column breakup is associated with the bag/shear aerodynamic mechanism similar to the breakup of nonturbulent liquid jets in cross flow. More study is needed, however, to resolve breakup lengths for the numerous practical applications where $\rho_f/\rho_g < 500$.

Perhaps the most important issues that need to be considered for turbulent liquid breakup involve effects of nonuniform and partially developed turbulence at the jet exit, information about the rates of liquid atomization along the liquid surface and more complete understanding about aerodynamic effects on drop velocities after turbulent primary breakup and liquid breakup lengths for $\rho_f/\rho_g < 500$.

Nonturbulent Primary Breakup

Introduction

The second example of primary breakup will address round liquid jets in gaseous cross flows. This atomization configuration is of interest due to applications to airbreathing propulsion systems, liquid

rocket engines, diesel engines, spark ignition engines and agricultural sprays, among others. It is likely that many of these applications actually involve turbulent, or partly turbulent and nonuniform, liquid jets in cross flows. Unfortunately, quantitative information about effects of turbulence on the breakup of liquid jets in cross flow, comparable to liquid jets in still gases, is not available; therefore, present considerations will be limited to the classical configuration of a nonturbulent liquid jet in nonturbulent gaseous cross flows.

There have been numerous studies of liquid jets in gaseous cross flows that have concentrated on penetration lengths and jet/spray plume trajectories for various liquid properties, liquid jet properties and cross flow properties, see Wu et al.[65] and references cited therein. The primary breakup properties of liquid jets in cross flow have recently received more attention, with Wu et al.[65], Vich and Ledoux[66] and Mazallon et al.[67] reporting striking similarities between the breakup properties of round liquid jets in gaseous cross flows and the secondary breakup of drops. The studies of Wu et al.,[65] and Vich and Ledoux[66] however, involve considerable uncertainties about flow uniformity and turbulence levels at the jet exit; therefore, the following discussion will focus on the observations of Mazallon et al.[67] where jet exit and cross flow turbulence conditions were well defined. The following discussion will be limited to the definition of breakup regimes and associated liquid column disturbance properties (waves) due to lack of information about other aspects of breakup, e.g., outcomes, dynamics, etc.

Breakup Regimes

The measurements of Mazallon et al.[67] involved nonturbulent round liquid jets in uniform cross flows of air at STP (having turbulence intensities less than 2%). Liquid injection was accomplished by pressure atomization using either round sharp-edged (Borda) nozzles or round supercavitating nozzles (having a sharp-edged inlet and exit with $L/d < 3$). Both injector configurations yielded uniform nonturbulent liquid jets, with smooth surfaces and no tendency to break up similar to liquid cutting jets, in the absence of cross flow. Test conditions involved various liquids, liquid jet diameters of 0.8-13 mm, liquid jet velocities of 0-50 m/s and air cross flow velocities of 0-24 m/s at STP.

For conditions where effects of liquid viscosity were small ($Oh < 0.1$), five kinds of flow were observed as the cross flow velocity (characterized by We) was increased: (1) simple deformation of the shape and trajectory of the liquid jet with no primary breakup, (2) breakup of the liquid column as a whole, (3) bag breakup, (4) bag/shear (multimode-like) breakup and (5) shear breakup. The bag, bag/shear (multimode) and shear breakup processes were qualitatively quite similar to the corresponding breakup regimes for secondary drop breakup discussed earlier. The main difference involved the appearance of thickened regions (nodes) along the liquid column which formed separations between similar breakup elements, e.g., bags. Flow behavior was qualitatively similar for $Oh > 0.1$ but long ligaments formed from the liquid column during breakup. The presence of long ligaments complicated measurements, therefore, no results were obtained for $Oh > 0.3$.

Exploiting the similarities between the primary breakup regimes of nonturbulent round liquid jets (liquid jets) in cross flow, and the secondary breakup of drops, mean jet primary breakup regimes were correlated in terms of We and Oh similar to the approach illustrated in Fig. 1 for the secondary breakup of drops. The resulting breakup regime map is illustrated in Fig. 13. The four liquid jet breakup regimes plotted in Fig. 13 are analogous to the secondary breakup regimes of drops subjected to shock-wave disturbances. In order to show this relationship, the secondary breakup regime map for drops from Hsiang and Faeth,[12-14] see Fig. 1, is plotted in Fig. 13 for comparison with the primary breakup regime map. The main difference between liquid column and drop breakup are that drop breakup does not have any behavior corresponding to liquid column breakup and that drop breakup responds more to increasing Oh than liquid jet breakup. The main breakup regimes for the liquid jets at $Oh < 0.1$ are as follows: liquid column breakup ($We < 5$), bag breakup ($5 < We < 60$), bag/shear breakup ($60 < We < 110$) and shear breakup ($110 < We$). Similar to other properties of liquid jet breakup, the liquid/gas momentum ratio, q, had little effect on the breakup regime map (for q of 100-8000).

Another feature of liquid jet breakup in cross flow was the appearance of waves along the liquid column. Two kinds of waves were observed: the wavelengths between nodes, λ_c, involving deflection

of the entire liquid column, and the smaller wavelength, λ_s, associated with periodic disturbances of liquid stripping along the sides of the liquid column during shear breakup. When normalized by the liquid jet diameter, these wavelengths were largely correlated with the Weber number and were relatively independent of Oh and q.

Normalized liquid column and liquid surface wavelengths are plotted as a function of the Weber number in Fig. 14. For reference purposes, values of We at transition to the various breakup regimes are also marked in the plots. Liquid column waves first appear in the liquid column breakup regime and eventually are associated with the disturbances that lead to breakup of the liquid column itself. These disturbances begin with $\lambda_c/d_o \approx 10$ at We ≈ 1 and then decrease to $\lambda_c/d_o \approx 1$ at We ≈ 60, which is comparable to wavelengths of surface waves, at the onset of the bag/shear breakup regime. These column type disturbances decrease at large We were the breakup process becomes dominated by shear breakup along the sides of the jet. The surface disturbance wavelengths are smaller than the liquid column waves, with λ_s/d_o generally less than unity. The wavelength of surface waves also decreases as We increases but they remain visible in shear breakup regime where they are associated with the distance between ligaments being stripped from the sides of the liquid columns.

Other available information about primary breakup of nonturbulent liquid jets in cross flow included deformation properties of the liquid column, and times of onset of liquid breakup.[47] Clearly, much more must be learned, however, in order to gain a reasonable understanding of this primary breakup process.

Conclusions

Aspects of primary breakup nonturbulent round liquid jets in gaseous cross flows have been reviewed, emphasizing air cross flows at STP ($\rho_f/\rho_g >$ 500). The main conclusions are as follows:

1. There is a useful general analogy between primary breakup of nonturbulent liquid jets in cross flow and the secondary breakup of individual drops which suggests modest streamwise interactions between cross-sections in the jets, e.g., liquid surface deformation and breakup properties are not strongly affected by the liquid/gas momentum flux ratio for values less than 8000, the largest value considered during past work.

2. Transitions to various breakup regimes are not influenced significantly by liquid viscosities for Oh < 0.1. For these conditions, the onset of breakup occurs as bag breakup at We = 5, the onset of bag/shear breakup occurs at We = 60 and the onset of shear breakup occurs at We = 110. Conditions for the onset of liquid column breakup are not known due to limited cross flow widths during past work.

3. The primary breakup process involved the formation of both column and surface waves. The wavelengths of both waves decrease with increasing We and they were relatively independent of Oh and q. The bag and bag/shear breakup regimes involved the presence of both types of waves but the liquid column breakup regime involved only the presence of column waves and the shear breakup regime involved only surface waves. An interesting feature of these results is that the wavelengths of column waves are roughly equal to the initial diameter of the jet at the onset of the shear breakup regime.

Available results about primary breakup of liquid jets in cross flow are clearly very limited. Properties, such as outcomes, dynamics, rates of liquid breakup, effects of liquid turbulence and effects of ρ_f/ρ_g and large Oh, among others, all remain to be resolved in order to provide the technology base needed to develop and model this primary breakup process.

Acknowledgments

The author's research on sprays has been supported by the U.S. Air Force Office of Scientific Research, Grant Nos. F49620-92-J-0399, F49620-95-1-0364 and F49620-99-1-0083 under the technical management of J. M. Tishkoff, U.S. Office of Naval Research, Grant Nos. N00014-85-J-1199 and N00014-95-J-0234 under the technical management of E. W. Rood and G. D. Roy and the Renault Research Division under the technical management of D. Lahalle and T. Mantel.

References

[1]Giffen, E., and Muraszew, A., *The Atomization of Liquid Fuels*, Wiley, New York, 1953.

[2]Hinze, J.O., "Fundamentals of the Hydrodynamic Mechanism of Splitting in Dispersion Processes." AIChE J., Vol. 1, 1955, pp. 289-295.

[3]Harrje, D.T., and Reardon, F.H., "Liquid Rocket Combustion Instability," NASA SP-194, 1972, pp. 49-55.

[4]Clift, R., Grace, J.R., and Weber, M.E., *Bubbles, Drops and Particles*, Academic Press, New York, 1978, pp. 26 and 339-347.

[5]Wierzba, A., and Takayama, K. "Experimental Investigation of the Aerodynamic Breakup of Liquid Drops," AIAA J., Vol. 26, 1988, pp. 1329-1335.

[6]Lefebvre, A.H., *Atomization and Sprays*, Hemisphere Publishing Co., New York, 1989, pp. 27-78 and 201-272.

[7]Faeth, G.M., "Structure and Atomization Properties of Dense Turbulent Sprays," Twenty-Third Symposium (International) on Combustion, The Combustion Institute, Pittsburgh, 1990, pp. 1345-1352.

[8]Wu, P.-K., Hsiang, L.-P., and Faeth, G.M., "Aerodynamic Effects on Primary and Secondary Breakup," Prog. Astro. Aero., Vol. 169, 1995, pp. 247-279.

[9]Faeth, G.M. Hsiang, L.-P., and Wu, P.-K., "Structure and Breakup Properties of Sprays," Int. J. Multiphase Flow, Vol. 21 (Suppl.), 1995, pp. 99-127.

[10]Tseng, L.-K., Ruff, G.A., Wu, P.-K., and Faeth, G.M., "Continuous- and Dispersed-Phase Structure of Pressure Atomized Sprays," Prog. Astro. Aero., Vol. 171, 1996, pp. 3-30.

[11]Faeth, G.M., "Spray Combustion Phenomena," Twenty-Sixth Symposium (International) on Combustion, The Combustion Institute, Pittsburgh, 1996, pp. 1593-1612.

[12]Hsiang, L.-P., and Faeth, G.M., "Near-Limit Drop Deformation and Secondary Breakup," Int. J. Multiphase Flow, Vol. 18, 1992, pp. 635-652.

[13]Hsiang, L.-P., and Faeth, G.M., "Drop Properties After Secondary Breakup," Int. J. Multiphase Flow, Vol. 19, 1993, pp. 721-735.

[14]Hsiang,L.-P., and Faeth, G.M., "Drop Deformation and Breakup due to Shock Wave and Steady Disturbances," Int. J. Multiphase Flow, Vol. 21, 1995, pp. 545-560.

[15]Chou, W.-H., Hsiang, L.-P., and Faeth, G.M., "Temporal Properties of Secondary Drop Breakup in the Shear Breakup Regime," Int. J. Multiphase Flow, Vol. 23, 1997, pp. 651-669.

[16]Chou, W.-H., Hsiang, L.-P., and Faeth, G.M., "Temporal Variation of Secondary Drop Breakup in the Bag Breakup Regime," Int. J. Multiphase Flow, Vol. 24, 1998, pp. 889-912.

[17]Dai, Z., and Faeth, G.M., "Temporal Properties of Secondary Breakup in the Multimode Breakup Regime," Int. J. Multiphase Flow, submitted.

[18]Hanson, A.R., Domich, E.G., and Adams, H.S., "Shock-Tube Investigation of the Breakup of Drops by Air Blasts," Phys. Fluids, Vol. 6, 1963, pp. 1070-1080.

[19]Gel'fand, B.E, Gubin, S.A., and Kogarko, S.M., "Various Forms of Drop Fractionation in Shock Waves and Their Special Characteristics," Inzhenerno-Fizicheskii Zhurnal, Vol. 27, 1974, 119-126.

[20]Krzeczkowski, S.A., "Measurement of Liquid Droplet Disintegration Mechanisms," Int. J. Multiphase Flow, Vol. 6, 1980, pp. 227-239.

[21]Ranger, A.A., and Nicholls, J.A., "The Aerodynamic Shattering of Liquid Drops," AIAA J., Vol. 7, 1969, pp. 285-290.

[22]Borisov, A.A., Gel'fand, B.E., Natanzon, M.S.. and Kossov, O.M.,"Droplet Breakup Regimes and Criteria for Their Existence," Inzhenerno-Fizicheskii Zhurnal, Vol. 40, 1981, pp. 64-70.

[23]Loparev, V.P., "Experimental Investigation of the Atomization of Drops of Liquid under Conditions

of a Gradual Rise of the External Forces," Izvestiya Akademii Nauk SSSR, Mekhanika Zhidkosti i Gaza, Vol. 3, 1975, pp. 174-178.

[24]Lane, W. R., "Shatter of Drops in Streams of Air," Ind. Engr. Chem., Vol. 43, 1951, pp. 1312-1317.

[25]Liang, P.Y., Eastes, T.W., and Gharakhari, A., "Computer Simulations of Drop Deformation and Drop Breakup," AIAA Paper No. 88-3142, 1988.

[26]Simpkins, P.G., and Bales, E.J., "Water-Drop Response to Sudden Accelerations," J. Fluid Mech., Vol. 55, 1972, pp. 629-639.

[27]Engel, O.G., "Fragmentation of Waterdrops in the Zone Behind an Air Shock," J. Res. Natl Bureau Stds., Vol. 6, 1958, pp. 245-280.

[28]White, F.M.,*Viscous Fluid Flow*, McGraw-Hill, New York, 1974.

[29]Simmons, H.C. "The Correlation of Drop-Size Distributions in Fuel Nozzle Sprays," J. Engr. for Power, Vol. 99, 1977, pp. 309-319.

[30]Merrington, A.C., and Richardson, E.G., "The Break-Up of Liquid Jets," Proc. Phys. Soc. (London), Vol. 59, 1947, pp. 1-13.

[31]Ryan, R.T., "The Behavior of Large Low-Surface-Tension Water Drops Falling at Terminal Velocity in Air," J. Appl. Meterology, Vol. 15, 1976, pp. 157-165.

[32]Hu, S., and Kintner, R.C., "The Fall of Single Drops Through Water," AIChE J., Vol. 1, 1955, pp. 42-48.

[33]De Juhasz, K.J., Zahn, O.F., Jr., and Schweitzer, P.H., "On the Formation and Dispersion of Oil Sprays," Engineering Experimental Station, Bulletin No. 40, Pennsylvania State University, University Park, PA, 1932, pp. 63-68.

[34]Lee, D.W., and Spencer, R.C., "Preliminary Photomicrographic Studies of Fuel Sprays," NACA Tech. Note 424, 1932.

[35]Lee, D.W., and Spencer, R.C., "Photomicrographic Studies of Fuel Sprays," NACA Tech. Note 454, 1933.

[36]Chen, T.-F. and Davis, J.R., "Disintegration of a Turbulent Water Jet," J. Hyd. Div., Vol. 1, 1964, pp. 175-206.

[37]Grant, R.P., and Middleman, S., "Newtonian Jet Stability," AIChE J., Vol. 12, 1966, pp. 669-678.

[38]Phinney, R.E., "The Breakup of a Turbulent Jet in a Gaseous Atmosphere," J. Fluid Mech., Vol. 60, 1973, pp. 689-701.

[39]Hiroyasu, H., Shimizu, M., and Arai, M., "The Breakup of a High Speed Jet in a High Pressure Gaseous Environment," ICLASS-82, Univ. of Wisconsin, Madison, 1982.

[40]Chehroudi, B., Onuma, Y., Chen, S.-H., and Bracco, F.V., "On the Intact Core of Full Cone Sprays," SAE Paper No. 850126, 1985.

[41]Ruff, G.A., Sagar, A.D., and Faeth, G.M., "Structure and Mixing Properties of Pressure-Atomized Sprays," AIAA J., Vol. 27, 1989, pp. 901-908.

[42]Ruff, G.A., Bernal, L.P., and Faeth, G.M., "Structure of the Near-Injector Region of Non-Evaporating Pressure-Atomized Sprays," J. Prop. Power, Vol. 7, 1991, pp. 221-230.

[43]Ruff, G.A., Wu, P.-K., Bernal, L. P., and Faeth, G.M. "Continuous- and Dispersed-Phase Structure of Dense Non-evaporating Pressure-Atomized Sprays," J. Prop. Power, Vol. 8, 1992, pp. 280-289.

[44]Tseng, L.-K., Ruff, G.A., and Faeth, G.M.. "Effects of Gas Density on the Structure of Liquid Jets in Still Gases," AIAA J., Vol. 30, 1992, pp. 1537-1544.

[45]Tseng, L.-K., Wu, P.-K., and Faeth, G.M., "Dispersed-Phase Structure of Pressure-Atomized Sprays at Various Gas Densities," J. Prop. Power, Vol. 8, 1992, pp. 1157-1166.

[46]Hoyt, J.W., and Taylor, J.J., "Waves on Water Jets," J. Fluid Mech., Vol. 88, 1977, pp. 119-123.

[47]Hoyt, J.W., and Taylor, J.J. "Turbulence Structure in a Water Jet Discharging in Air," Phys. Fluids, Vol. 20, 1977, pp. S253-S257.

[48]Wu, P.-K., Ruff, G.A., and Faeth, G.M., "Primary Breakup in Liquid/Gas Mixing Layers for Turbulent Liquids," Atom. Sprays, Vol. 1, 1991, pp. 421-440.

[49]Wu, P.-K., Tseng, L.-K., and Faeth, G.M., "Primary Breakup in Gas/Liquid Mixing Layers for Turbulent Liquids," Atom. Sprays, Vol. 2, 1992, pp. 295-317.

[50]Wu, P.-K., and Faeth, G.M., "Aerodynamic Effects on Primary Breakup of Turbulent Liquids," Atom. Sprays, Vol. 3, 1993, pp. 265-289.

[51]Wu, P.-K., and Faeth, G.M., "Onset and End of Drop Formation Along the Surface of Turbulent Liquid Jets in Still Gases," Physics of Fluids A, Vol. 7, 1995, pp. 2915-2917.

[52]Wu, P.-K., Miranda, R.F., and Faeth, G.M., "Effects of Initial Flow Conditions on Primary Breakup of Nonturbulent and Turbulent Round Liquid Jets," Atom. Sprays, Vol. 5, 1995, pp. 175-196.

[53]Dai, Z., Hsiang, L.-P., and Faeth, G.M., "Spray Formation at the Free Surface of Turbulent Bow Sheets," Proc. 21st Symp. on Naval Hydrodynamics, National Academy Press, Washington, D.C., 1997, pp. 490-505.

[54]Dai, Z., Chou, W.-H., and Faeth, G.M., "Drop Formation due to Turbulent Primary Breakup at the Free Surface of Plane Liquid Wall Jets," Phys. Fluids, Vol. 10, 1998, pp. 1147-1157.

[55]Dai, Z., Sallam, K.A., and Faeth, G.M., "Turbulent Primary Drop Breakup from Free Bow Sheets," Proc. 22nd Symp. on Naval Hydrodynamics, National Academy Press, Washington, D.C., in press.

[56]Sallam, K.A., Dai, Z., and Faeth, G.M., "Drop Formation at the Surface of Plane Tubulent Liquid Jets in Still Gases," Int. J. Multiphase Flow, in press.

[57]Sallam, K.A., Dai, Z., and Faeth, G.M., "Breakup of Turbulent Liquid Jets in Still Gases," AIAA Paper No. 99-3759, 1999.

[58]Schlichting, H., *Boundary Layer Theory*, 7th ed., McGraw-Hill, New York, 1979, pp. 599.

[59]Hinze, J.O., *Turbulence*, 2nd ed., McGraw-Hill, New York, 1975, pp. 427 and 724-734.

[60]Tennekes, H., and Lumley, J.L., *A First Course in Turbulence*, MIT Press, Cambridge, Massachusetts, 1972, pp. 248-286.

[61]Karasawa, T., Tanaka, M., Abe, K., Shiga, S., and Kurabayashi,T., "Effects of Nozzle Configuration on the Atomization of a Steady Spray," Atom. Sprays, Vol. 2, 1992, pp. 411-426.

[62]Yokota, M., Ito, Y., and Shinoke, T., "High Speed Photographic Observations of Cavitation Arising in the High-Speed Oil-Flow Through a Very Small Long Orifice," 9th Intl. Symp. on Jet Cutting Tech., Sendai, 1988, pp. 13-21.

[63]Levich, V.G., *Physicochemical Hydrodynamics*, Prentice-Hall, Inc., Englewood Cliffs, NJ, 1962, pp. 639-646.

[64]Taylor, G.I., "Generation of Ripples by Wind Blowing Over a Viscous Liquid," *The Scientific Papers of Sir Geoffrey Ingram Taylor*, G.K. Batchelor, ed., Vol. III, Cambridge University Press, Cambridge, 1963, pp. 244-254.

[65]Wu, P.-K., Kirkendall, K.A., Fuller, R.P., and Nejad, A.S., "Breakup Processes of Liquid Jets in Subsonic Crossflows," J. Prop. Power, Vol. 13, 1997, pp. 64-73.

[66]Vich, G., and Ledoux, M., "Investigation of a Liquid Jet in a Subsonic Cross-Flow," ICLASS-97, Seoul, 1997, pp. 23-30.

[67]Mazallon, J., Dai,Z., and Faeth, G.M., "Primary Breakup of Nonturbulent Round Liquid Jets in Gas Crossflows," Atom. Sprays, in press.

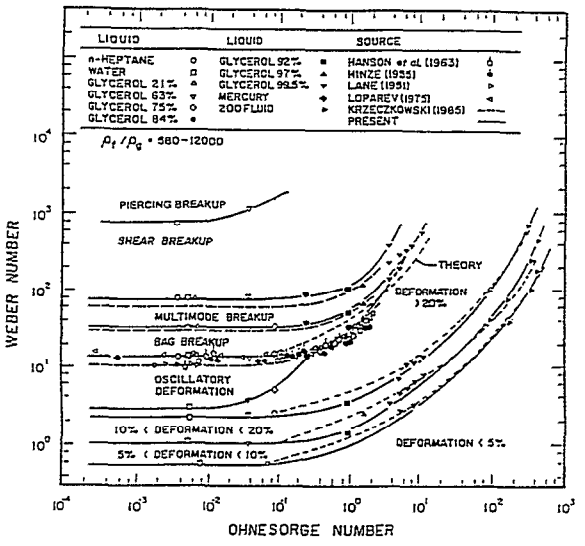

Fig. 1 Drop formation and secondary breakup regime map for shock-wave disturbances and $\rho_f/\rho_g > 500$. From Chou et al.[15] with measurements from Hansen et al.,[18] Hinze,[2] Lane,[24] Loparev[23] and Hsiang and coworkers;[12-14] correlations from Krczkowski[20] and Hsiang and coworkers;[12-14]; theory from Hsiang and Faeth.[14]

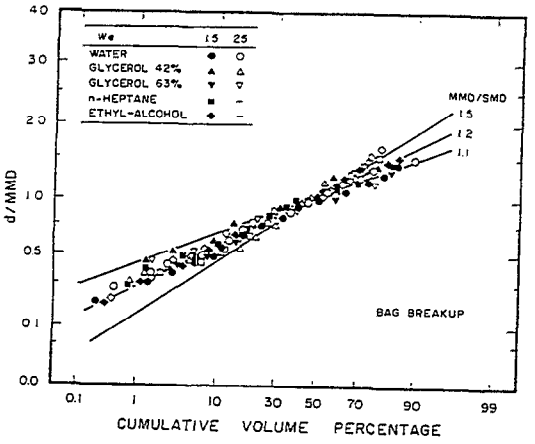

Fig. 2 Distribution of drop diameters after bag breakup. From Hsiang and Faeth.[12]

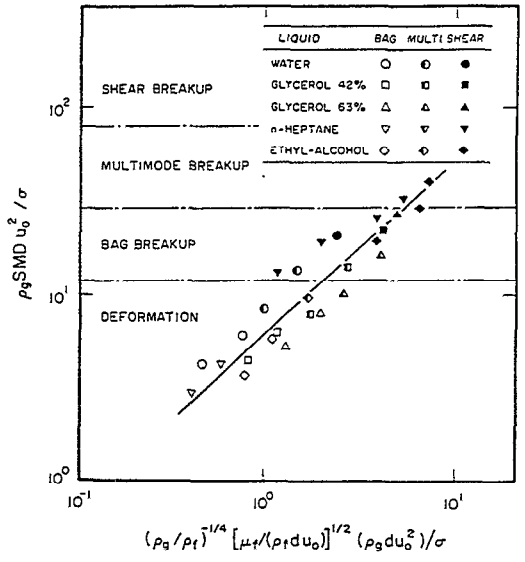

Fig. 3 Correlation of SMD after secondary breakup for shock-wave disturbances for $\rho_f/\rho_g > 500$. From Hsiang and Faeth.[12]

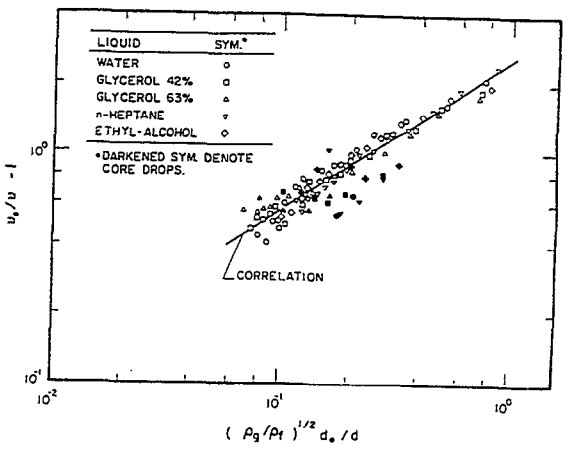

Fig. 4 Correlation of drop velocities after secondary breakup for shock-wave disturbances for $\rho_f/\rho_g > 500$. From Hsiang and Faeth.[13]

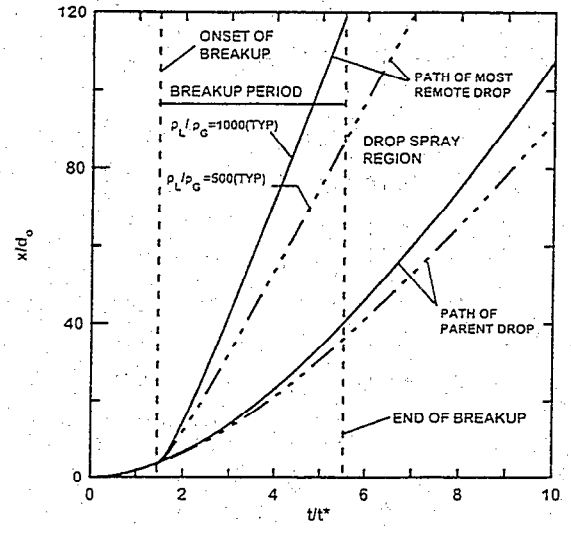

Fig. 5 Growth of the spray-containing region during shear breakup for $\rho_f/\rho_g > 500$. From Chou et al.[15]

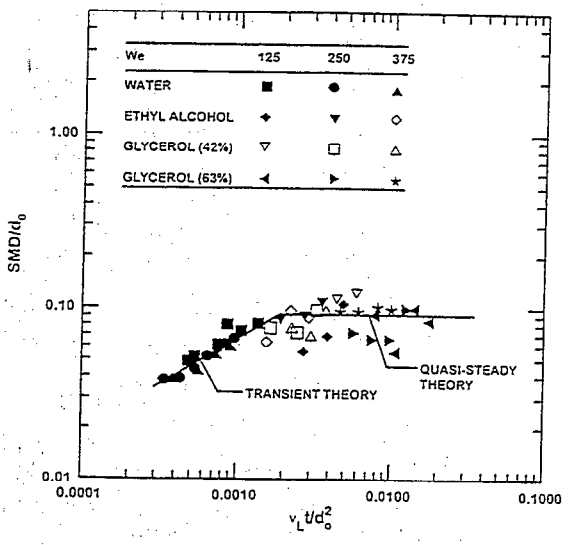

Fig. 6 Temporal variation of the SMD of drops produced by shear breakup for $\rho_f/\rho_g > 500$. From Chou et al.[15]

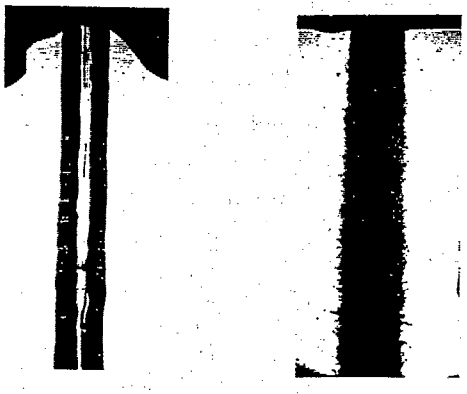

Fig. 7 Pulsed shadowgraphs of water jets injected into still air at NTP with nonturbulent slug flow at the jet exit and with and without boundary layer removal. From Wu et al.[52]

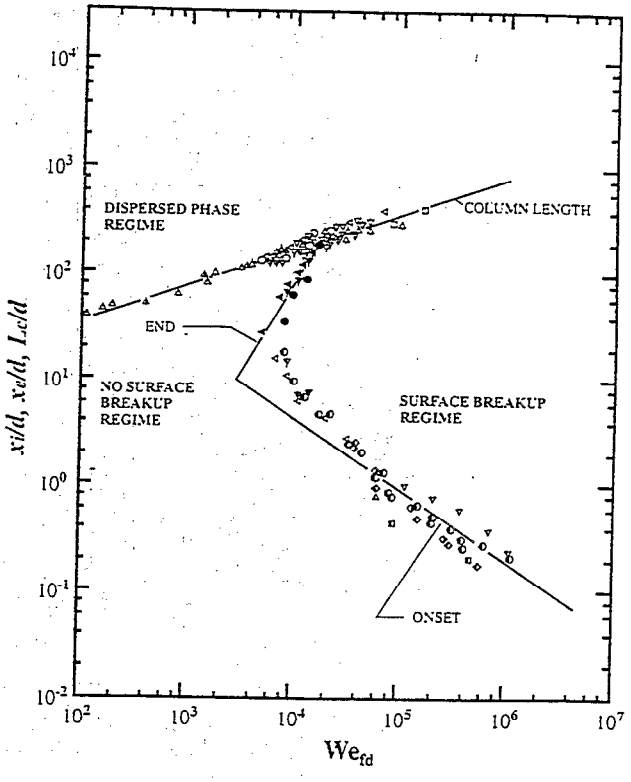

Fig. 8 Liquid-surface and liquid-column breakup regime maps for liquid jets injected into still gases with fully-developed turbulent pipe flow at the jet exit and negligible aerodynamic effects. From Wu and Faeth,[51] with measurements from Chen and Davis,[36] Grant and Middleman,[37] Wu and Faeth,[51] and Wu et al.[52].

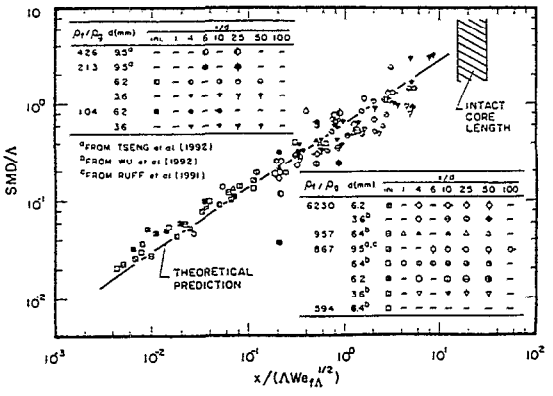

Fig. 9 SMD after turbulent primary breakup as a function of distance from the jet exit for liquid jets injected into still gases with fully-developed turbulent pipe flow at the jet exit. Results for $\rho_f/\rho_g <$ 500 inverted to account for merged primary and secondary breakup. From Wu and Faeth,[50] with measurements from Ruff et al.,[42] Tseng et al.,[44] Wu and Faeth,[51] and Wu et al.[52] SMD predictions from Wu and Faeth,[51] and liquid-column length prediction from Grant and Middleman.[37]

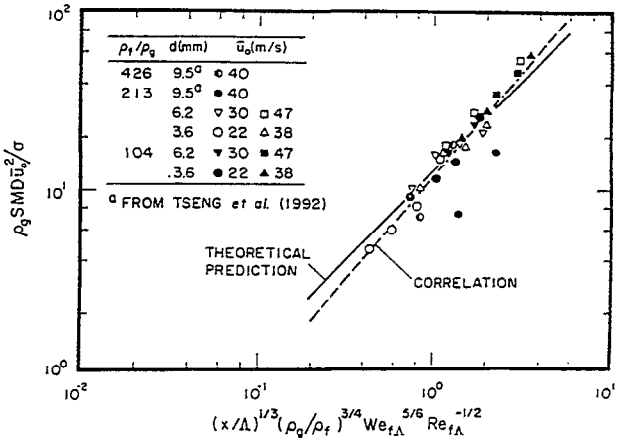

Fig. 10 SMD after aerodynamically enhanced turbulent primary breakup as a function of distance from the jet exit. From Wu and Faeth,[50] with measurements from Tseng et al.,[44] and Wu and Faeth;[50] SMD predictions from Wu and Faeth[50].

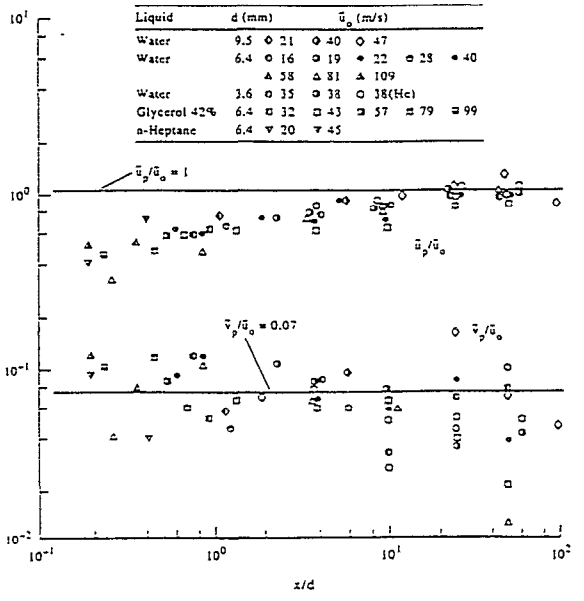

Fig. 11 Mass averaged drop velocities after turbulent primary breakup of round turbulent liquid jets as a function of distance from the jet exit. From Wu et al.[49]

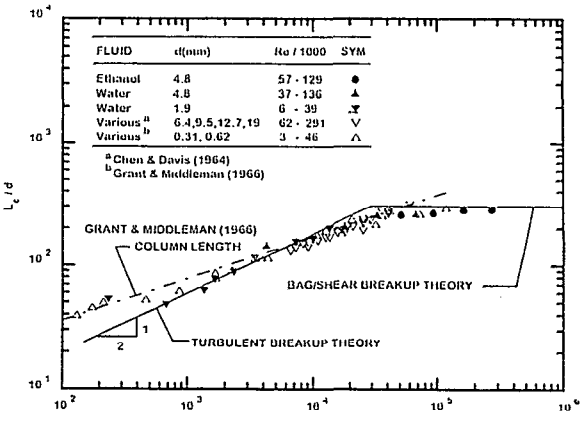

Fig. 12 Mean breakup length of round turbulent liquid jets in still air plotted according to the turbulent and bag/shear liquid column breakup theories. From Sallam et al.[56] Measurements of Chen and Davis,[36] Grant and Middleman[37] and Sallam et al.[57] Breakup length correlations of Grant and Middleman[37] and Sallam et al.[57]

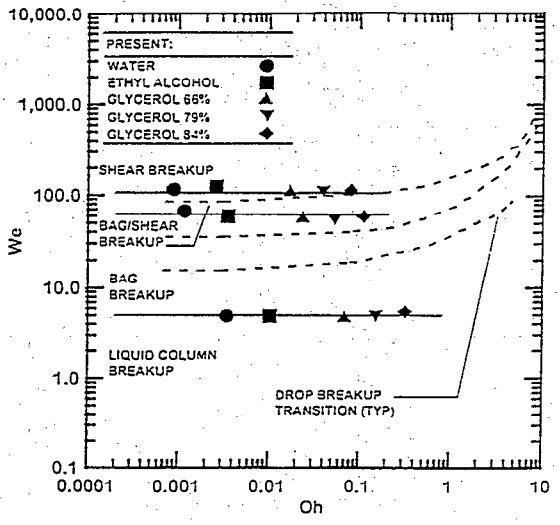

Fig. 13 Breakup regime maps for primary breakup of round nonturbulent liquid jets in gaseous cross flows from Mazallon et al.[67] and for the secondary breakup of drops from Hsiang and Faeth.[12] $\rho_f/\rho_g >$ 500.

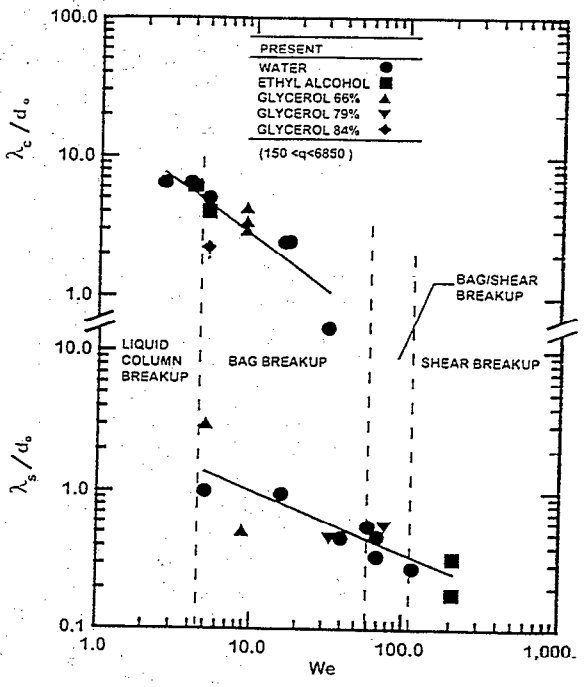

Fig. 14 Liquid column and surface wavelengths for nonturbulent round liquid jets in air cross flows. From Mazallon et al.[67]